Modeling the thermal behavior of solar salt in electrical resistance heaters for the application in PV-CSP hybrid power plants

Cite as: AIP Conference Proceedings **2445**, 030013 (2022); https://doi.org/10.1063/5.0086268
Published Online: 12 May 2022

Zahra Mahdi, Phani Srujan Merige, Ricardo Alexander Chico Caminos, et al.

Modeling the Thermal Behavior of Solar Salt in Electrical Resistance Heaters for the Application in PV-CSP Hybrid Power Plants

Zahra Mahdi[1, a)], Phani Srujan Merige[1], Ricardo Alexander Chico Caminos[1], Pascal Schmitz[1], Ulf Herrmann[1], Cristiano Teixeira Boura[1], Mark Schmitz[2], Hans Gielen[2], Yibekal Gedle[2], Jürgen Dersch[3]

[1]*Solar-Institut Jülich of the Aachen University of Applied Sciences (SIJ), Heinrich-Mussmann-Str. 5, 52428 Jülich, Germany.*
[2]*TSK Flagsol Engineering GmbH, Anna-Schneider-Steig 10, 50678 Köln, Germany.*
[3]*DLR Institute of Solar Research, Linder Höhe, 51147 Köln, Germany.*

[a)] Corresponding author: mahdi@sij.fh-aachen.de

Abstract. Concentrated Solar Power (CSP) systems are able to store energy cost-effectively in their integrated thermal energy storage (TES). By intelligently combining Photovoltaics (PV) systems with CSP, a further cost reduction of solar power plants is expected, as well as an increase in dispatchability and flexibility of power generation. PV-powered Resistance Heaters (RH) can be deployed to raise the temperature of the molten salt hot storage from 385 °C up to 565 °C in a Parabolic Trough Collector (PTC) plant. To avoid freezing and decomposition of molten salt, the temperature distribution in the electrical resistance heater is investigated in the present study. For this purpose, a RH has been modeled and CFD simulations have been performed. The simulation results show that the hottest regions occur on the electric rod surface behind the last baffle. A technical optimization was performed by adjusting three parameters: Shell-baffle clearance, electric rod-baffle clearance and number of baffles. After the technical optimization was carried out, the temperature difference between the maximum temperature and the average outlet temperature of the salt is within the acceptable limits, thus critical salt decomposition has been avoided. Additionally, the CFD simulations results were analyzed and compared with results obtained with a one-dimensional model in Modelica.

INTRODUCTION

Concentrated Solar Power (CSP) and Photovoltaics (PV) are the two main technologies to convert solar energy into electricity. Solar PV has already reached grid parity in many countries, but large scale electrical storage technologies are currently not available or relatively expensive. Thermal energy from concentrating collector systems, on the other hand, can be easily stored, and the conversion of heat into electricity can take place in line with demand in the conventional steam power block of the CSP system. However, electricity from CSP is currently more expensive than PV electricity, in case there are no additional incentives for storage. The smart integration of both technologies into a single hybrid system can lead to a cost-effective solution for flexible and reliable solar power production. [1,2]

Different PV-CSP configurations are currently developed in a number of projects, but so far, hybridization has been limited to a common feed from the separate systems into the power grid. [3,4] A more effective hybridization could be achieved by coupling the systems by means of a power to heat (P2H) unit (e.g. Resistance Heater (RH) or High Temperature Heat Pump (HT HP)) and by optimizing the integration of both systems. [2,3,5–7] The investigation of a RH for the integration in PV-CSP hybrid power plants is one of the main aims of the ongoing project SWS, which is carried out in cooperation between SIJ, TSK Flagsol and DLR.

SolarPACES 2020
AIP Conf. Proc. 2445, 030013-1–030013-8; https://doi.org/10.1063/5.0086268
Published by AIP Publishing. 978-0-7354-4195-8/$30.00

The only PV-CSP power plant designed as a fully integrated individual system is the “Noor Midelt I” project in Morocco, which has been announced in May 2019. The plant, which will have a total installed capacity of 800 MWel, is the world’s first fully hybrid PV-CSP power plant. [8]

APPROACH

Parabolic trough collector (PTC) systems commonly utilize thermal oil as heat transfer fluid (HTF) and operate with a maximum temperature of 393 °C. Molten salt allows higher operating temperatures, thus improving the power block efficiency of the system. RH can be deployed to raise the temperature of the molten salt hot storage to 565 °C in a PTC plant. A PV field can supply the power for the RH, therefore storing the PV electricity cost-effectively in the molten salt thermal storage. The molten salt is heated up in the RH to 565 °C after it has been preheated in an oil-salt heat exchanger to less than 393 °C. The salt is then stored in the thermal energy storage. A schematic diagram of such system is shown in Fig. 1.

The so-called solar salt is the most utilized commercial molten salt in CSP systems, and is also subject of the present study. Solar salt can be used over a temperature range of 260 °C to approximately 565 °C. As temperature decreases below this range, the salt crystallizes at 238 °C and as it increases beyond 565 °C, the salt starts to decompose and loses its thermal stability at about 600 °C [9]. Therefore, the goal of the present study is to investigate a resistance heater with molten salt in CFD simulations, to determine the temperature distribution and the occurrence of uneven heating areas, especially the hot spots. In the present study, a RH has been designed specifically for the application with solar salt for solar power plants and a series of CFD simulations have been performed to optimize it from a technical point of view.

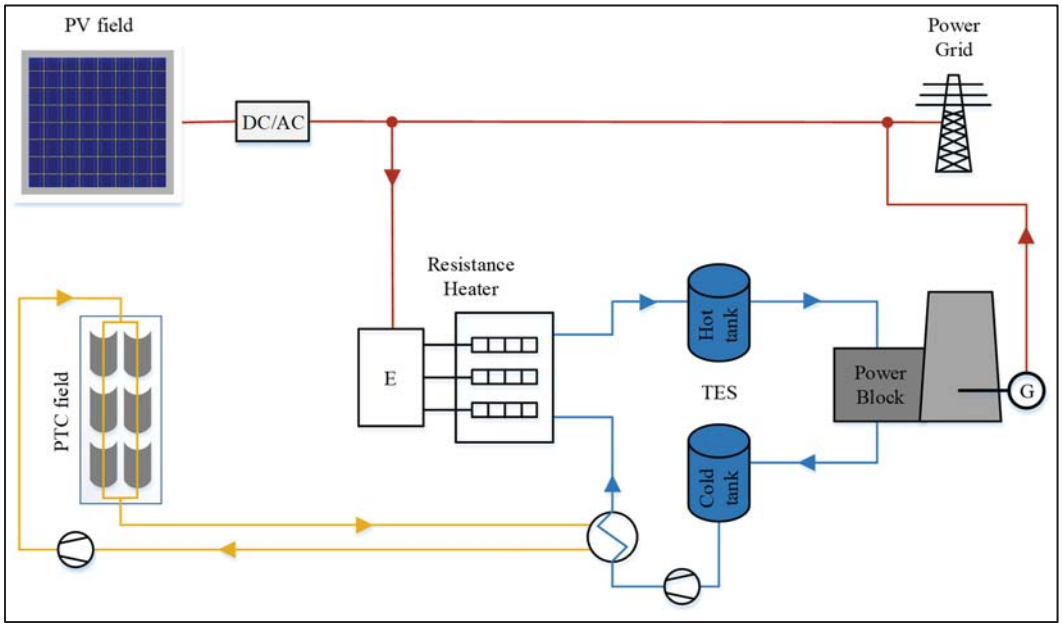

FIGURE 1. System configuration of a PV-CSP hybrid power plant together with TES and RH

MODELING AND SIMULATION

CFD Analysis

A 3D model of a RH was created and simulated in ANSYS® FLUENT. The left section in Fig. 2 shows the main components of an electric resistance heater in a cross-sectional view, whereas on the right side the arrangement and connections of electric rods and baffles along the RH length are illustrated.

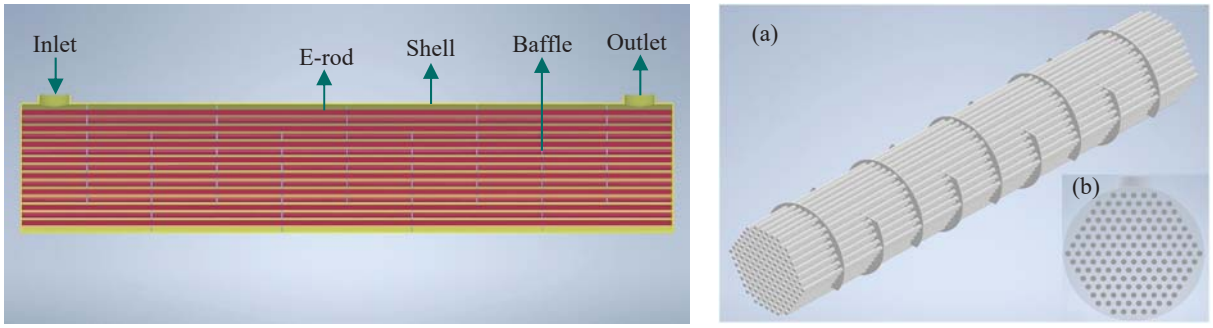

FIGURE 2. Left: Cross-sectional view of the electrical resistance heater; Right: (a) Isometric view of electric rods and baffles arrangement, (b) Front view of electric rods

The design of the RH is based on a shell and tube heat exchanger [10] in which the second fluid in the tubes is replaced by the electric rods. Baffles have been applied to increase the turbulence of the fluid flow. A power of 600 kW has been assumed for the model, which represents a rather small RH to avoid very large computing times. In this model, there are 150 e-rods and the RH has a length of 2 m. For simplification, the U-bends of the rods have not been considered in the simulations. The physical properties of the heating fluid are those of the solar salt (a mixture of 60 wt. % $NaNO_3$ and 40 wt. % KNO_3).

The surface load is assumed to be 40,000 W/m^2 and the mass flow rate of the salt is 20 kg/s to have a Reynolds number of approx. 10,000, which corresponds to a fully turbulent model. The outlet temperature was kept at 560 °C, so the inlet temperature has been calculated reversely for the reference model and then kept constant at 541.6 °C for all the rest. The term 'baffle cut' which is used to specify the dimensions of a segmental baffle, is the height of the segment removed to form the baffle and is expressed in percentage. In general, a baffle cut of 20-25% is considered optimum, to give good heat transfer rates without excessive pressure drop. [11] For the following simulations a baffle cut of 22% has been assumed.

In Tab. 1, the design parameters of the system are shown. The shell and the baffles are made of steel and the e-rods of incoloy-800.

TABLE 1. Basic design parameters of the RH model

Parameter	Value
No. of e-rods	150
Diameter of e-rod [mm]	16
Length of e-rod [mm]	2000
Tube bundle diameter [mm]	380
Shell inner diameter [mm]	392
Shell thickness [mm]	3.2
Shell outer diameter [mm]	398.4
Baffle diameter [mm]	390.4
Baffle cut [%]	22

The mesh element selected for the models is tetrahedron. These elements are highly adaptive to mesh refinement, fit better for a complex geometry and help capture small variations in fluid flow. The quality of the mesh has been evaluated with the parameters Aspect Ratio, Skewness and Orthogonal Quality. The Aspect Ratio and Skewness have a maximum value of 1.86 and 0.22 respectively and the Orthogonal Quality is approximately 0.76 for the models. The Y^+ is ca. 157.5. These values ensure an acceptable and good quality mesh for the models, which result in convergence of the simulations with high stability and accuracy. [12]

The models have been optimized according to three different design parameters:

1. Shell-baffle clearances (SBC) between 0.6 and 6.4 mm.
2. E-rod-baffle clearances (EBC) between 0.6 and 6.4 mm.
3. Number of baffles between 5 to 11.

The clearances are shown in Fig. 3 for a better understanding.

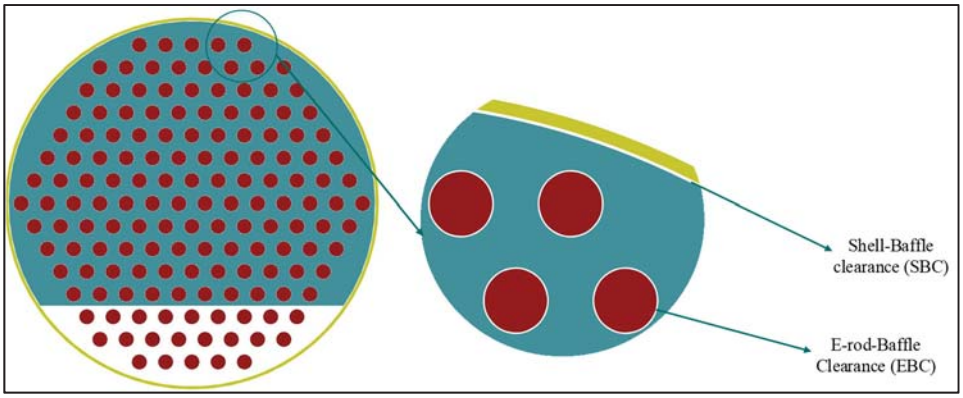

FIGURE 3. The magnified optimization parameters of SBC and EBC

The simulations have been performed for the 3D model for constant inlet temperatures and mass flow rates. For the outer surface of the electric rods, a shell conduction approach was applied with constant heat flow rates. The reference model has a value of 0.8 mm for both EBC and SBC and the number of baffles of 5. Therefore, for each parameter study, two of the values have been kept constant at the reference value and the third one has been swept. For all the simulations, the average outlet temperatures as well as the maximum reached temperature in the whole heater were compared. Up to this point, the optimization goal was to get as close as possible to the outlet temperature of 560 °C and minimize the maximum temperatures reached.

The results of the simulations for different EBC and SBC are shown in Fig. 4 (a) and (b), respectively.

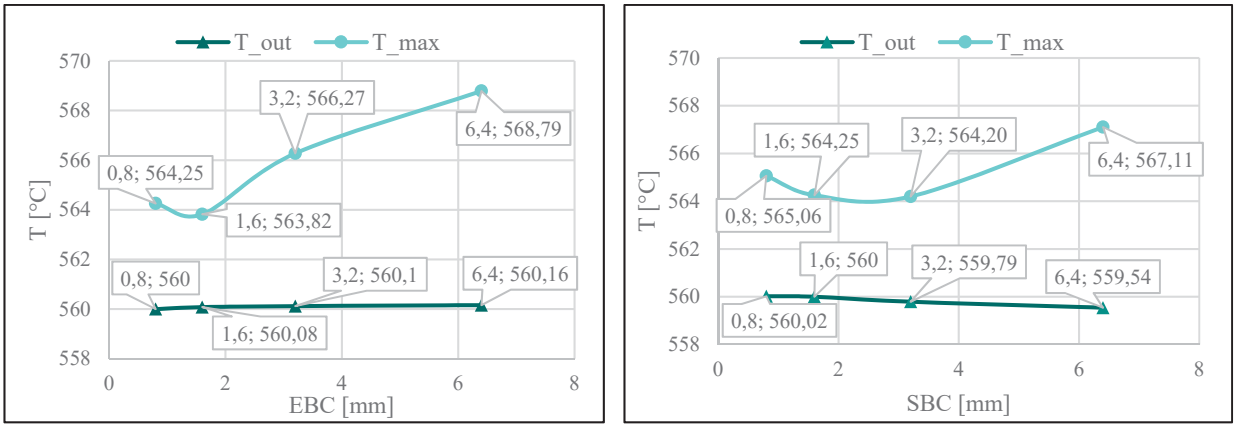

FIGURE 4. Optimization results of the simulations with different (a) EBC and (b) SBC

As it can be seen in Fig. 4 (a), for an EBC of 1.6 mm, the maximum temperature reached in the system has the smallest value, which is fulfilling the optimization aim. For smaller clearances, the hot spots occur behind the baffles and for larger EBC, the turbulences will not occur as expected.

For the simulation results in Fig. 4 (b), the maximum reached temperatures for the cases with a SBC of 1.6 and 3.2 mm show almost the same results, although for the case with a SBC of 3.2 mm, the outlet temperature has slightly dropped. For this reason, the case with 1.6 mm SBC has been chosen as the optimized case.

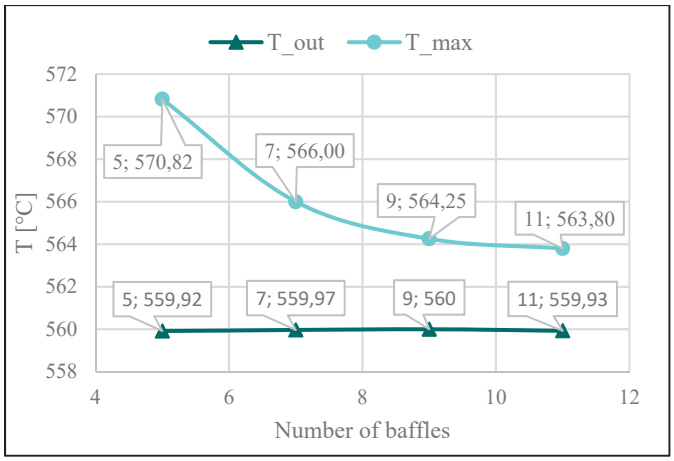

FIGURE 5. Optimization results of the simulations with different number of baffles

Figure 5 shows the results for the last case, i.e. the simulations with different number of baffles. As it can be seen, the maximum reached temperature is decreasing with increasing number of baffles, although the changes are becoming rather small. In order to verify the simulation model with a Dymola® model in the next step, it was necessary to keep the distances between the baffles constant. Therefore, it was not possible to simulate a larger number of baffles, as the baffles interfere with the inlet and outlet sectors. Hence, the model with 11 baffles has been chosen here as the optimized case.

Table 2 shows a summary of the optimization values together with the results of the simulation of the optimized model. The average outlet temperature in this case is almost 560 °C and the maximum reached temperature has a value of 563.37 °C. The average heat transfer coefficient is about 3000 W/m^{2}K and the pressure drop is in the acceptable range defined in [13].

TABLE 2. Values of the selected parameters of the optimized model

	Parameter	**Value**
Optimization value	EBC [mm]	1.6
	SBC [mm]	1.6
	No. of baffles	11
Results	T out [°C]	559.97
	T max [°C]	563.37
	h [W/m^{2}K]	3070.95
	Pressure drop [bar]	0.141

Figure 6 shows the temperature distribution of the optimized model. On the left side, an axial cross section in the middle of the heater is shown, whereas on the right side the radial cross section after the last baffle is illustrated. As it can be seen the maximum reached temperatures occur after the last baffle near the e-rods especially on the sides of the heater and where the baffle cut ends.

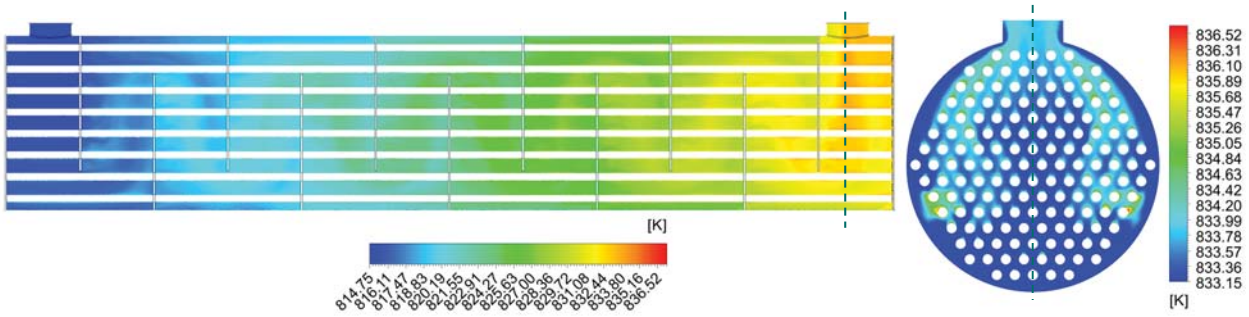

FIGURE 6. Temperature distribution of the molten salt in the heater from (left) axial cross section view and (right) radial cross section view

Model Verification

A detailed dynamic simulation model of the electric heater using the Modelica programming language in Dymola® has been developed to verify the CFD simulation results. The model combines the electrical, thermal and flow behavior of the electric heater and its individual components. Both, the CFD and the dynamic model complement each other and comparing the results allows a deeper understanding of the simulation outcomes.

Among other parameters, the model, which is primarily one-dimensional, can simulate the electrical power, the thermal power absorbed by the molten salt, the temperature profiles of the salt and electric rods along the length and the radial temperature distribution within the electric rods. To compute the temperature distributions in the radial direction, the model also includes 2D representations of the system. Each e-rod is built in three layers. The first layer represents the heating wire in the form of an electrical resistance, which is connected to two heat storage components and two thermal conductors from the standard Modelica library. Each pair of components corresponds to one additional layer of the e-rod. The second layer represents the electrical insulation and the last layer corresponds to the metal jacket. The heat transfer between the metal jacket of the e-rod and the molten salt takes place at last. The heat transfer coefficient h in the outer area of the tube bundle is calculated using the equations from Gaddis Gnielinski [11], which provide an average convective heat transfer coefficient based on correlations between baffle, shell and tube geometry.

The main geometry parameters of the investigated electric heater in ANSYS® FLUENT were imported into the Dymola® model and the steady state operation was simulated. The resulting average heat transfer coefficient, the Reynolds number and the salt outlet temperature were analyzed and compared to the results of the 3D CFD simulations.

Table 3 shows the relative deviation of the simulation results from the Dymola® model with respect to the CFD model for the optimized model. As seen in Tab. 3 the Reynolds number and the salt outlet temperature from the one-dimensional model show good agreement with the computed values in ANSYS® FLUENT. When comparing the h values the deviations show a value of 20.43 %, which is rather high. The large deviation is mainly due to the fact that the geometry of the resistance heater cannot be fully represented in the Dymola® model. For this reason, there is an uncertainty in some of the factors needed for calculating the heat transfer coefficient using the equations from [11], such as the geometry correction factor and the leakage correction factor. Additionally, there is another fact to be considered when comparing both simulation models. In the one-dimensional model, one value of h is calculated for each discretized section, whereas the heat transfer coefficient from ANSYS® is computed during post-processing by dividing the area weighted wall heat flux by the difference between the area weighted wall temperature and the wall adjacent temperature at the electric rods.

TABLE 3. Relative deviation of the simulated salt outlet temperature (Tout), Reynolds number (Re) and average heat transfer coefficient (h) between Modelica and CFD simulations

Optimized Model	Tout	Re	h
Relative Deviation [%]	0.27	0.69	20.43

Figure 7 shows the trend of the convective heat transfer coefficient along the length of the electric rod for the optimized model. It is evident from the figure that these coefficients are maximum in close proximity to the baffles.

One of the aims of the model comparison was to identify the largest sources of uncertainty within the models. The results from the CFD simulation will be utilized to further refine the dynamic simulation model in Dymola® to improve its accuracy. Experimental data will be needed to validate both models.

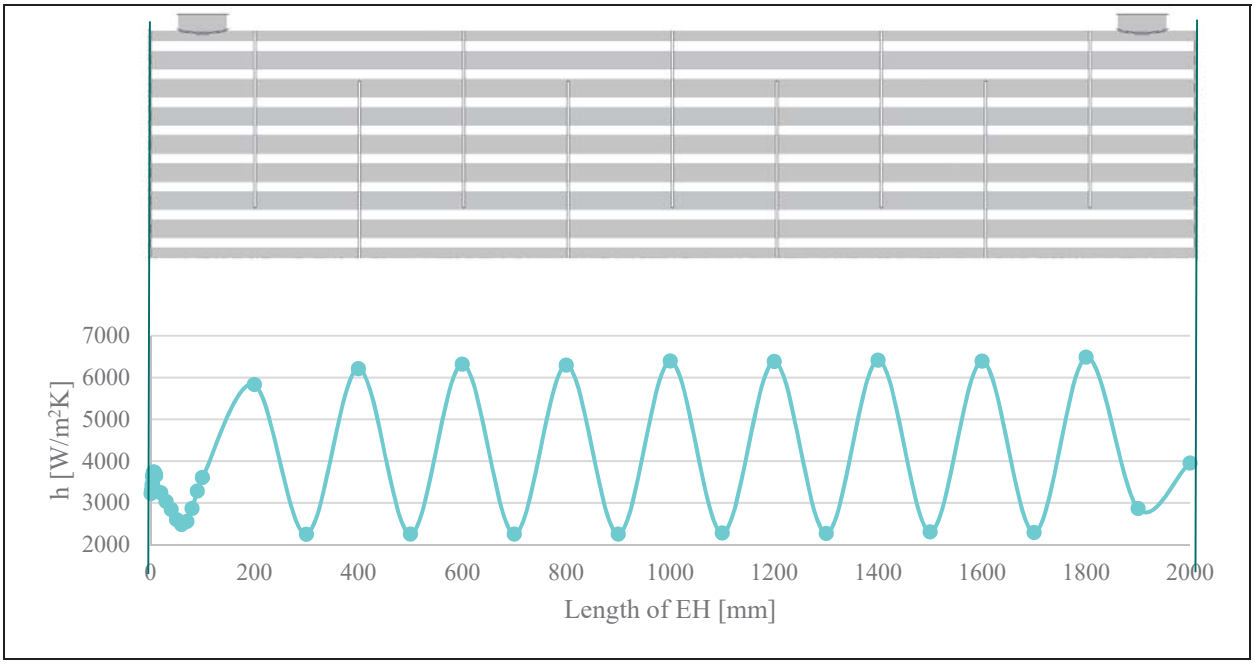

FIGURE 7. Trend of *h* along the length of the electric rod in the reference model

CONCLUSION AND OUTLOOK

A RH has been designed and optimized for the application in PV-CSP hybrid power plants with solar salt as the working fluid and storage medium. CFD simulations have been performed to optimize the model for different SBC, EBC and various number of baffles in order to reduce the inhomogeneity of the temperature distribution in the heater and to avoid the possible hot spots or dead zones along the e-rods in the heater.

Molten salt temperatures have been spotted after the last baffle, which were higher than the outlet temperatures. The maximum reached temperatures were found close to the electric rods in this region, although, the highest temperatures reached in the optimized model, have been less than the maximum allowed temperature for the solar salt. Hence, they don‘t cause any damages to the system. This means, with the optimized values of the clearances and the number of baffles, the dead zones and hot spots have been avoided behind the baffles.

The CFD simulation results have been compared with the detailed dynamic model in Dymola®. As the next milestone of the project, detailed simulations of the whole system including the PV, CSP, TES and also the discretized dynamic model of the RH are currently being performed at SIJ. The validation of the results with experimental data is in the framework of the ongoing project SWS.

ACKNOWLEDGMENTS

The authors gratefully acknowledge the financial support from the LeitmarktAgentur.NRW and the state government of North Rhine Westphalia.

REFERENCES

1. IRENA, *Renewable power generation costs in 2019*, <https://www.irena.org/-/media/Files/IRENA/Agency/Publication/2020/Jun/IRENA_Costs_2019_EN.pdf?la=en&hash=BFAAB4DD2A14EDA7329946F9C3BDA9CD806C1A8A>.

2. U. Herrmann, B. Kelly, and H. Price, Two-tank molten salt storage for parabolic trough solar power plants. Elsevier Ltd. 5-6 (2004).
3. HELIOCSP, *Dubai 950 MW Concentrated Solar Power +PV Noor Energy 1 breaks 8 world records*, <http://helioscsp.com/dubai-950-mw-concentrated-solar-power-pv-noor-energy-1-breaks-8-world-records/>.
4. KfW, *Solar Complex Ouarzazate - Morocco*. *Project information*, <https://www.kfw-entwicklungsbank.de/PDF/Entwicklungsfinanzierung/Themen-NEU/Projekt-Marokko-Solar-2016-EN.pdf>.
5. Agora Energiewende, Power-to-Heat zur Integration von ansonsten abgeregeltem Strom aus Erneuerbaren Energien, Studie (2014).
6. D. Böttger, Auswirkungen von Power-to-Heat-Anlagen in der Fernwärmeversorgung in Deutschland. 10. Internationale Energiewirtschaftstagung an der TU Wien (2017).
7. M. Schwarzenbart, M. Sauerborn, S. Dittmann, and U. Herrmann, Stromspeicher I-TESS, Studie zur Integration thermischer Stromspeicher in existierende Kraftwerksstandorte. Solar-Institut Jülich (2017).
8. S. Kraemer, *Morocco Breaks New Record with 800 MW Midelt 1 CSP-PV at 7 Cents*, <https://www.solarpaces.org/morocco-breaks-new-record-with-800-mw-midelt-1-csp-pv-at-7-cents/>.
9. Thomas Bauer, *Verfahren zur Überwachung der Flüssigsalzqualität und Betriebserfahrung mit der TESIS-Anlage* (Köln, 2018).
10. J. Bonilla, A. de La Calle, M. M. Rodríguez-García, L. Roca, and L. Valenzuela, Study on shell-and-tube heat exchanger models with different degree of complexity for process simulation and control design. Applied Thermal Engineering (2017).
11. E. S. Gaddis and V. Gnielinski in *VDI heat atlas* (Springer-Verlag Berlin Heidelberg, Berlin, 2010), p. 731.
12. K. Ho-Le, Finite element mesh generation methods: a review and classification. Computer-Aided Design 1 (1988).
13. R. K. Sinnott, J. M. Coulson, and J. F. Richardson, *Coulson & Richardson's chemical engineering*. *Vol. 6: Chemical engineering design*, 4th ed. (Elsevier Butterworth-Heinemann, Oxford, 2005).